

Thermionic field emission from nanocrystalline diamond-coated silicon tip arrays

J. M. Garguilo,* F. A. M. Koeck, and R. J. Nemanich

Department of Physics, North Carolina State University, Raleigh, North Carolina 27695-8202, USA

X. C. Xiao, J. A. Carlisle, and O. Auciello

Materials Science Division, Argonne National Laboratory, Argonne, Illinois 60439, USA

(Received 23 April 2005; revised manuscript received 21 July 2005; published 4 October 2005)

Thermionic field emission properties of nitrogen doped ultrananocrystalline diamond (UNCD) coated silicon tip arrays are examined using thermionic field emission electron microscopy (TFEEM). Nitrogen doping has been shown to enhance the emission properties of diamond by the introduction of a donor level 1.7 eV below the conduction band minimum. The field enhancing geometry of the films initiates accelerated electron emission at the tipped structures which may be beneficial to thermionic energy converter design where space charge effects can significantly limit attainable current densities. Two temperature regimes of electron emission are observed; 600–800 °C, where the emission is enabled because of the H passivation and 900–1100 °C, where the emission is attributed to tunneling from nitrogen related states through the barrier of a clean diamond surface.

DOI: [10.1103/PhysRevB.72.165404](https://doi.org/10.1103/PhysRevB.72.165404)

PACS number(s): 73.63.Bd

I. INTRODUCTION

This study investigates the thermionic field emission properties of ultrananocrystalline diamond (UNCD) films in field enhancing geometries through the use of field emission electron microscopy (FEEM) and thermionic field emission electron microscopy (TFEEM). Thermionic field emission has been described by a modified Richardson-Dushman equation¹ given by

$$J(E, T) = A_R T^2 e^{-\varphi - \sqrt{e^3 E/k_B T}}, \quad (1)$$

where the current density $J(E, T)$ is dependent on the work function, φ , the temperature of the emitter T and the applied electric field E at the surface, and A_R is the Richardson constant, e the electron charge, and k_B is the Boltzmann's constant. The introduction of sharp surface features creates a focusing of the electric field at the protruding surface. This enhanced field results in two effects, a narrower tunnel barrier and a reduction in the potential barrier (i.e., the Schottky effect).

Studies involving thermionic energy converters have suggested that crystalline carbon films in combination with field enhancing properties may be promising candidates for the emitting material.² Thermionic energy conversion is accomplished through the combination of a hot electron emitter in conjunction with a somewhat cooler electron collector. In operation, an electric potential will develop between the two surfaces that can result in a significant source of electrical energy. The system directly converts the thermal energy into electrical energy, and since the process is based on electron emission and collection with no mechanical motion, this source can be highly efficient and also operate without maintenance for extended periods of time. A limiting phenomenon to the vacuum emission of electrons is the space charge effect in which electrons in the vacuum close to the emitter surface impede additional electron emission. A potential method to reduce this limiting effect is the introduction of

surface features that produce a field enhancement effect at the surface. The electrons emitted from the tip shaped surface features are rapidly accelerated, and the transit time from the emitter to the electron collector is reduced, consequently reducing the space charge effects.

Field enhancement through the introduction of surface features has been studied for many years, most notably with sharp metal tips.^{3,4} The Fowler-Nordheim equation, which describes field emission from a metal surface, is often modified with a field enhancement factor β to reflect the influence of surface topography on electron emission. Research on metal tips has focused in part on producing self-collimated, coherent electron beams and has resulted in tips with a single atom at their apex.⁵⁻⁷ It has been proposed that the field emission from these structures would be nearly independent of temperature up to several hundred degrees Celsius.⁸ The temperatures of the prior studies were well below the temperatures examined in this study where thermionic emission predominates over field emission. Additional testing with silicon tips has been completed by several groups and similar results have been reported.^{9,10} In contrast to these studies, the results described here exploit the moderate enhancement from a robust, easily producible tip array in contrast to the extremely sharp tips employed for narrow energy range electron sources.

Ultrananocrystalline diamond films have been deposited by microwave plasma-enhanced chemical-vapor deposition using either a C60/Ar or CH₄(1%)/Ar plasma that lead to the generation of C₂ molecular precursors.¹¹ These precursors result in the growth of films with 2–5 nm grain sizes and 0.3–0.4-nm-wide grain boundaries. Results indicate that UNCD is predominately diamond phase material with less than 5% of the film graphitic or amorphous phase as indicated by selected-area electron diffraction.¹² The presence of the sp^2 bonds suggests that carbon is π bonded at the grain boundaries. UNCD films exhibit a number of interesting materials properties, including enhanced field emission, and electrochemical, as well as mechanical, tribological, and

conformal coating properties suitable for micro-electro-mechanical system devices.^{11,13}

Electron emission microscopy can be used to image the electron emission properties of a surface in a controlled UHV environment. In this system, electrons emitted from the surface are accelerated through a potential of 20 kV and imaged with electron optics. This instrument can be operated in a number of different configurations in order to investigate electron emission originating from various mechanisms. In its most basic mode, termed field-emission electron microscopy, the potential difference between the sample and anode is the only mechanism which enables electron emission. At a sufficient applied electric field the potential barrier width is reduced making quantum-mechanical tunneling of electrons into the vacuum possible. Illuminating the sample with UV light (from a mercury arc lamp) is termed photoelectron emission microscopy (PEEM). PEEM uses the photoelectric effect to assist the ejection of electrons from the sample. In this case, the electrons are emitted above the vacuum potential. The apparatus is capable of sample temperatures up to 1200 °C. True thermionic emission occurs when there is no applied field. This process involves thermally excited electrons which are emitted over the potential barrier at the surface and into the vacuum. The operation of the electron emission microscope requires a potential difference between the sample and the anode in order to direct the emitted electrons through the lens column. Therefore, imaging electrons at elevated temperatures is termed thermionic-field emission electron microscopy (TFEEM).

We have previously used electron imaging techniques to examine emission from relatively flat N-doped polycrystalline films.^{14,15} PEEM measurements of our MPCVD N-doped polycrystalline diamond films show uniform emission over the whole sample surface with a fine textured grainy structure that is similar to SEM images. No detectable field emission below 400 °C is observed for these flat films. As the temperature is increased, very uniform electron emission can be observed that increases in intensity with increasing temperature. Heating above ~900 °C results in a significant decrease in emission attributed to the loss of hydrogen from the surface and an increase in the electron affinity. Previous studies of conformally coated UNCD tips showed room temperature field emission at turn on fields as low as 1 V/ μm with minimal dependence on coating thickness or tip geometry.¹¹ However, the films in this study exhibit behavior similar to our previously examined N-doped polycrystalline diamond films and do not exhibit field emission at room temperature.

II. EXPERIMENTAL DETAILS

The preparation of the samples for this study consisted of three separate steps: substrate preparation, pretreatment, and growth of the UNCD film. The silicon tip array was patterned using conventional photolithography and etching techniques, producing ~1 μm tall tips spaced ~2.5 μm apart. The pretreatment portion of sample preparation first consisted of the deposition of a thin molybdenum layer over the entire substrate. The 10 nm metal film was deposited by

magnetron sputtering with an rf power of 100 Watts in an Ar environment of 10^{-2} Torr. This metal layer was intended to assist in the seeding of the substrate and to enhance the nucleation density of the diamond film. The substrate was then seeded ultrasonically in a solution of methanol and nanodiamond powder for 30 min. UNCD growth was carried out in a microwave plasma assisted CVD chamber. The gas concentrations during growth were 99% Ar, 10% N₂, and 1% CH₄ at a temperature of 800 °C and a microwave power of 1200 W. The deposition time was for 20 min resulting in an expected film thickness of 100 nm.

Before and after the thermal experiments, each sample was examined with Raman spectroscopy and scanning electron microscopy (SEM) in order to confirm the film structure and to monitor any change due to the annealing process. Visible Raman spectroscopy was first performed with a Renishaw Raman microscope in the backscattering geometry with a HeNe laser at 633 nm and an output power of 25 mW focused to a spot size of about 2 mm. A Hitachi s-4700 field emission scanning electron microscope with an accelerating voltage of 10 kV was used to image the preannealed samples. Post anneal samples were imaged with a JEOL Model JSM-6400F.

PEEM and FEEM measurements were carried out in an Elmitec UHV photoelectron emission microscope. The field of view of the instrument can be varied between 1.5 and 150 μm with a resolution less than 15 nm and a base pressure of 1×10^{-10} Torr. A high voltage of 20 kV was applied between the anode and the sample surface in order to accelerate the emitted electrons through the electron optics of the microscope. The distance between the anode and sample surface was between 2 and 4 mm resulting in an applied field of between 10 and 5 V/ μm . Electrons emitted from the sample pass through a perforated anode and are imaged with a fluorescent screen. A microchannel plate between the fluorescent screen and electron optics intensifies the image and a CCD camera records the data. In the PEEM measurements, a mercury arc lamp was used as the UV light source. When the light source was turned off and the emission is solely from the high applied field, the emission mode was termed FEEM. Sample heating up to 1200 °C is also available in the system and, when employed, the measurements are termed TPEEM or TFEEM, depending on the use (or lack of) photoexcitation in congruence with thermal excitation.

III. RESULTS

Raman spectra of the films are shown in Fig. 1. The shape of the spectra obtained from the nitrogen doped UNCD films is similar to those of nanocrystalline diamond. There are several identifiable peaks, the *D*-band peak at ~1340 cm^{-1} , the *G*-band peak at ~1556 cm^{-1} , and an undetermined shoulder at 1140 cm^{-1} often associated with nanocrystalline diamond. The *D* and *G* band peaks are attributed to sp^2 -bonded carbon while the 1140 cm^{-1} peak has been attributed to sp^2 -bonded carbon, nanocrystalline diamond, or transpolyacetylene segments at grain boundaries and surfaces.¹⁶⁻¹⁸

SEM images of the tip array and the individual tip structure are shown in Fig. 2. From these images, it is evident that

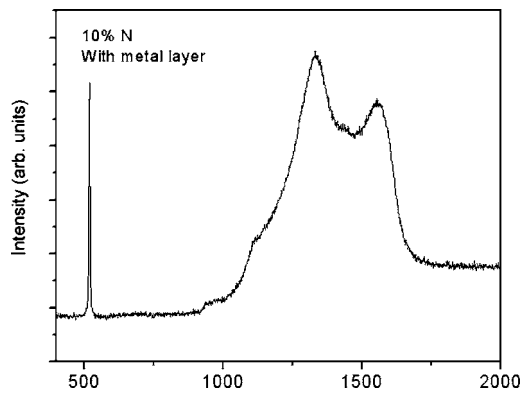


FIG. 1. Raman spectra of the UNCD coated tip array before annealing show characteristics peaks associated with nanocrystalline diamond. The *D*-band peak at ~ 1340 cm^{-1} , the *G*-band peak at ~ 1556 cm^{-1} , and a slight shoulder at ~ 1140 cm^{-1} are identifiable. The sharp peak at ~ 520 cm^{-1} is of the underlying silicon.

the UNCD film has completely covered the substrate and the tip structures. The tips themselves can be estimated to have a diameter of ~ 100 nm and a height of 1 μm yielding a geometric field enhancement factor (h/r) of approximately 20. SEM images before and after the thermal experiments are also shown. No change in tip structure, geometry or composition is detectable after annealing to over 1000 $^{\circ}\text{C}$.

A PEEM image of the UNCD tip array film at room temperature is shown in Fig. 3. The image was obtained with UV excitation from an Hg arc discharge lamp with a cutoff at ~ 5.1 eV. The image indicates photoemission from both the tip structures and the flat background of the film. The emission is enhanced at the tips apparently due to the increased local field. The photoexcited electrons in the conduction band of the diamond are emitted into vacuum due to the negative electron affinity (NEA) of the film. Prior research has shown that the (100), (110), and (111) surfaces of dia-

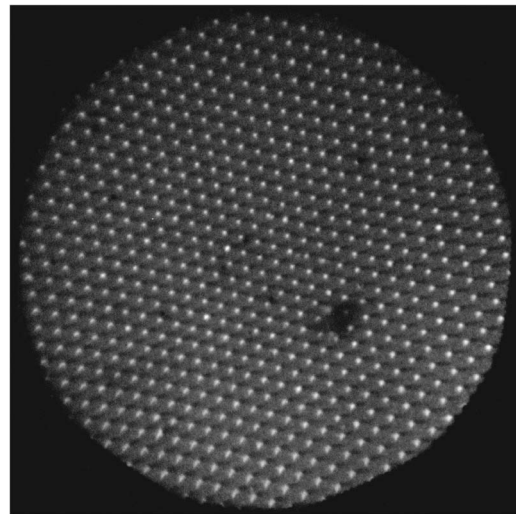


FIG. 3. A PEEM image of the UNCD coated tip array at room temperature. Emission is evident from both the flat areas of the sample and the tipped structures. Field of view is 150 μm .

mond exhibit a NEA when terminated with hydrogen.^{19–24} For a film with a negative electron affinity, the vacuum level is pulled below the conduction band minimum (CBM) at the surface. Electrons excited into the conduction band will be released into vacuum without having to overcome an additional energy barrier.

At room temperature, very low intensity FEEM images were only detectable when the CCD camera was integrated for 30 s. The very weak emission is attributed to noise and artifacts of the measuring system. As the sample was heated above 600 $^{\circ}\text{C}$, electron emission became evident. Temperature dependent FEEM images from 800 to 830 $^{\circ}\text{C}$ are shown in Fig. 4. Significant detectable emission was observed at 800 $^{\circ}\text{C}$ with emission originating from both the tip structures and the flat background of the film, similar to the PEEM imaging. An increase in the emission intensity is observed with increasing temperature up to 830 $^{\circ}\text{C}$ whereby there is significant degradation of the emission which we attribute to the loss of the film's NEA due to the desorption of the hydrogen. These results are consistent with our prior studies of nitrogen doped polycrystalline diamond films.^{14,15} After the desorption of hydrogen from the surface, the emission from most locations significantly decreases in intensity.

As the temperature is increased further, a second regime of emission becomes evident starting around 900 $^{\circ}\text{C}$, as shown in Fig. 5. Electron emission from several tips is clearly resolved and an increase in the number of emitting tips, as well as intensity, is observed with increasing temperature. Interestingly, emission is no longer detectable from the relatively flat background of the sample. The emission site density increases up to 1050 $^{\circ}\text{C}$ when almost all of the tips in the array are detectable. A further increase in temperature may have resulted in damage to the imaging system and, as such, was not explored. This high-temperature regime is attributed to thermionic tunneling from N-defect states through the lowered potential barrier of the tips. The field enhancing geometry of the tips results in enhanced tunneling at the higher temperatures. Unlike the initial thermionic field

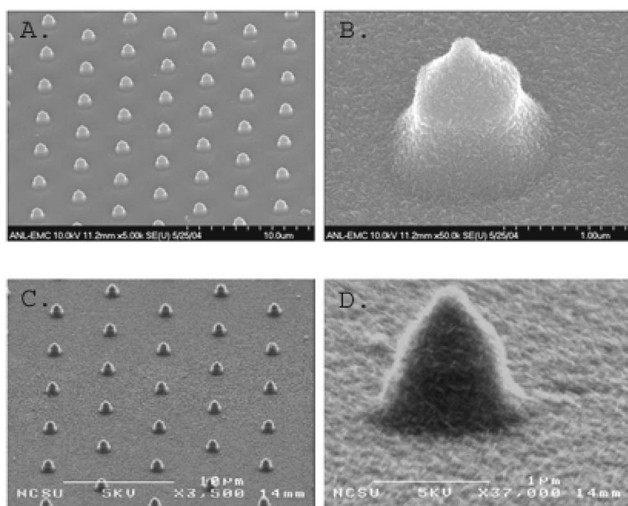


FIG. 2. SEM of the UNCD coated Si array before annealing indicates tips which are completely coated with the UNCD film (A and B). The diameter of the tip is approximately 100 nm while the height is 1 μm . SEM after the annealing experiments (C and D) shows no change in coverage, shape, or structure of the film.

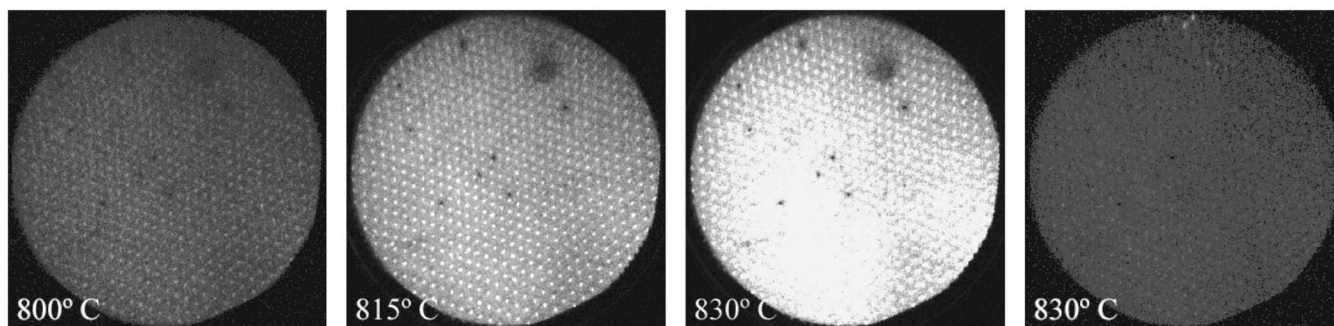


FIG. 4. Temperature dependent FEEM images of the UNCD coated tip array. A steady increase in electron emission with increasing temperature is observed up to 830 °C. Electron emission is detectable from both the tips and flat background of the sample. The geometric field enhancement effect results in stronger emission from the apex of the tips as compared to the background. After five minutes of exposure at the elevated temperature, the emission degrades. This corresponds to a loss in the film's NEA due to hydrogen evolution from the surface. Field of view is 150 μm .

emission, this second regime does not rapidly degrade with time. Several temperature sweeps were conducted in which the sample was cooled to approximately 850 °C and reheated to 1050 °C. The emission characteristics were stable in both intensity and density of emission sites. Unfortunately, the present setup does not allow for emission current measurements of specific regions of the samples.

IV. DISCUSSION

The presence of geometric structures on the surface of the film complicates the explanation of the electron emission. The barrier in a simplified vacuum potential approximation can be expressed by the equation

$$V(z) = - (e^2/4z) - eEz \quad (2)$$

which applies for $z > 0$.²⁵ In Fig. 6 this expression is plotted against the band diagram expected for nitrogen doped crystalline diamond materials possessing both negative and positive electron affinities. The electron affinities for the given diamond surfaces were taken to be -1.3 eV for the hydrogen terminated surface²⁶ and $+0.7$ eV for the hydrogen desorbed surface.²⁷ Nitrogen doping has been shown to result in donor states 1.7 eV below the conduction band,²⁸ and diamond has

a band gap of 5.5 eV. We have assumed flat bands at the surface.

The barrier lowering due to the local field at the tip and flat surface can be calculated using

$$V_{\text{max}} = -3.79E^{1/2} \text{ eV}, \quad (3)$$

where E is in units of $\text{V}/\text{\AA}$ and V_{max} is equal to 0.53 and 0.12 eV below the vacuum level, respectively.²⁵ Using our experimentally applied field and the geometric enhancement, the maximum potential barrier is determined to be 0.41 eV less than that at the flat surface. In the case of hydrogen passivation, in which the film possesses a negative electron affinity [Fig. 6(a)], when electrons from either the tipped or flat surfaces of the sample are thermally excited into the conduction band, they experience no additional potential barrier and are emitted into the vacuum. As the temperature is increased, the number of emitted electrons, and the intensity of emission, increases.

However, the adsorbed hydrogen layer has been shown to be unstable at elevated temperatures.¹⁴ Once these temperatures are reached, the hydrogen desorbs and the electron affinity is increased to a positive value of 0.7 eV [Fig. 6(b)]. The conduction band minimum is then located below the vacuum level and, in the absence of an applied electric field,

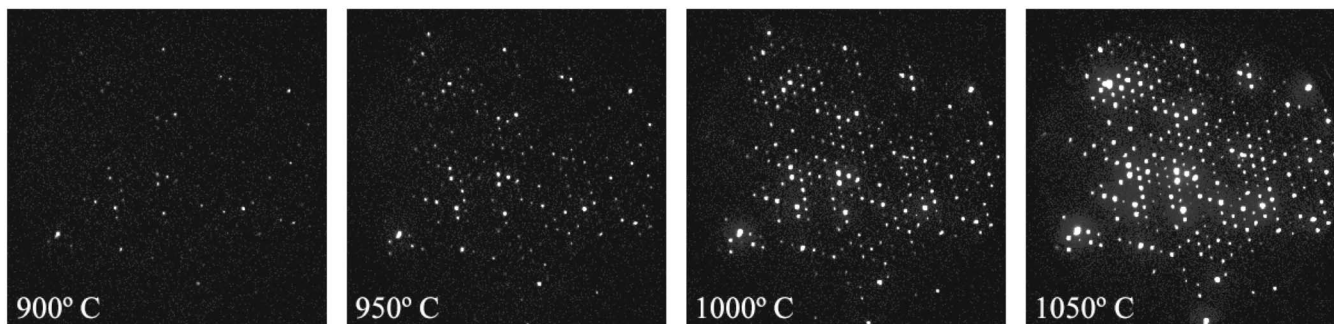


FIG. 5. Temperature dependent FEEM images of the UNCD coated tip array at elevated temperatures. After the loss of the film's NEA, temperature dependent field emission continues to be evident. As the sample is annealed to higher temperatures, strong electron emission is observed from the tips of the array, and there is no longer detectable emission from the flat background of the sample. This emission is stable and repeats with successive increasing and decreasing temperature sweeps. Field of view is 150 μm .

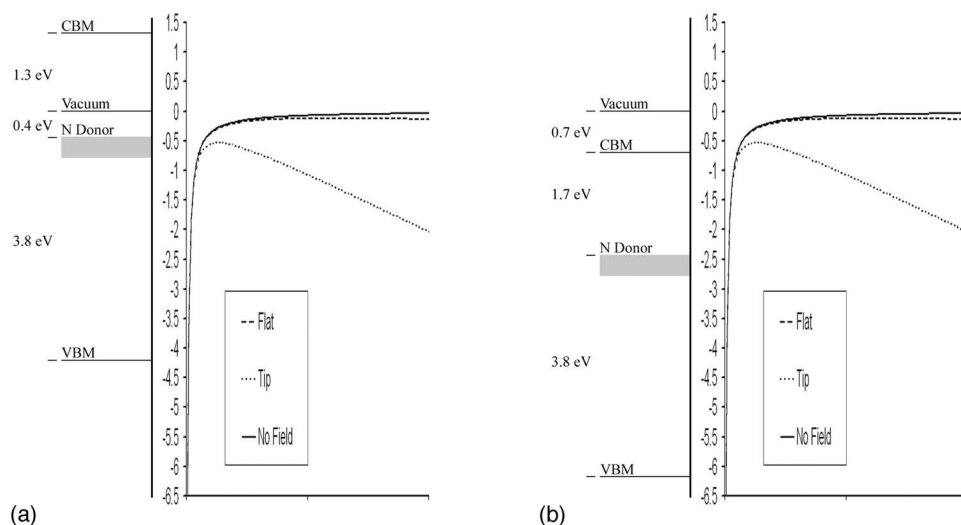


FIG. 6. The potential barriers of the geometric features of the film are plotted versus the band diagram of nitrogen doped diamond for the case of a -1.3 eV electron affinity (NEA) (a), and a $+0.7$ eV electron affinity (PEA) (b).

electrons occupying this energy level experience an additional potential barrier inhibiting their emission.

The electron emission characteristics of the UNCD coated tip array film make it a candidate for inclusion in future thermionic energy converting devices. The film shows spatially controllable emission (i.e., uniform over the deposited area) at relatively low temperatures as compared to conventional thermionic emitters. The field enhancing geometry would accelerate the emitted electrons more rapidly across the vacuum gap and thereby reduce space charge effects.

V. CONCLUSIONS

The electron emission at elevated temperatures from UNCD coated tip arrays has been examined with TFEEM. The electron emission characteristics of the film are consistent with other polycrystalline, nitrogen doped diamond films at moderate temperatures.^{14,15} The emission consists of a uniform increase in intensity with increasing temperature due to the negative electron affinity of the surface. Because of the geometric structure, i.e., tipped surface, field enhancement

effects enhance the emission at the protrusions. At a temperature of ~ 800 °C, the hydrogen passivation desorbs from the surface of the film and the NEA is lost. This results in an overall decrease in the emission intensity. With increasing temperature, emission is again observed from the tipped structures. This second regime is stable upon annealing sweeps. The field enhancing geometry of the sample results in a barrier lowering as predicted by the Fowler-Nordheim equation. This barrier lowering, along with the ability to counteract space charge effects, makes the field enhancing geometry a promising candidate for thermionic energy converting devices.

ACKNOWLEDGMENTS

We gratefully acknowledge the Duke University Free Electron Laser Laboratory where all of the field electron emission microscopy experiments were performed. This research work was supported in part by the ONR MURI on Thermionic Energy Conversion and the ANL DOE CESP Program.

*Corresponding author. Electronic address: jmgargui@ncsu.edu

¹W. Schottky, Phys. Z. **15**, 872 (1914).

²F. A. M. Koeck, J. M. Garguilo, R. J. Nemanich, S. Gupta, B. R. Weiner, and G. Morell, Diamond Relat. Mater. **12**, 474 (2003).

³P. C. Bettler and F. M. Charbonnier, Phys. Rev. **119**, 85 (1960).

⁴J. W. Gadzuk and E. W. Plummer, Rev. Mod. Phys. **45**, 487 (1973).

⁵H.-W. Fink, Phys. Scr. **38**, 260 (1988).

⁶V. T. Binh and N. Garcia, Ultramicroscopy **42–44**, 80 (1992).

⁷V. T. Binh, S. T. Purcell, N. Garcia, and J. Doglioni, Phys. Rev. Lett. **69**, 2527 (1992).

⁸K. R. Shoulders, *Advances in Computers*, edited by F. L. Alt (Academic, New York, 1961), Vol. 2, pp. 135–293.

⁹C. E. Hunt, J. T. Trujillo, and W. J. Orvis, IEEE Trans. Electron Devices **38**, 2309 (1991).

¹⁰H. H. Busta, B. J. Zimmerman, J. E. Pogemiller, M. C. Tringides, and C. A. Spindt, J. Vac. Sci. Technol. B **11**, 400 (1993).

¹¹A. R. Krauss, O. Auciello, M. Q. Ding, D. M. Gruen, Y. Huang, V. V. Zhirnov, E. I. Givargizov, A. Breskin, R. Chechen, E. Shefer, V. Konov, S. Pimenov, A. Karabutov, A. Rakhimov, and N. Suetin, J. Appl. Phys. **89**, 2958 (2001).

¹²J. Birrell, J. E. Gerbi, O. Auciello, J. M. Gibson, D. M. Gruen, and J. A. Carlisle, J. Appl. Phys. **93**, 5606 (2003).

¹³O. Auciello, J. Birrell, J. A. Carlisle, J. E. Gerbi, X. C. Xiao, B. Peng, and H. D. Espinosa, J. Phys.: Condens. Matter **16**, R539 (2004).

¹⁴F. A. M. Kock, J. M. Garguilo, Billyde Brown, and R. J. Nemanich, Diamond Relat. Mater. **11**, 774 (2002).

¹⁵F. A. M. Kock, J. M. Garguilo, and R. J. Nemanich, Diamond Relat. Mater. **10**, 1714 (2001).

- ¹⁶A. C. Ferrari and J. Robertson, *Phys. Rev. B* **63**, 121405(R) (2001).
- ¹⁷J. Birrell, J. E. Gerbi, O. Auciello, J. M. Gibson, J. Johnson, and J. A. Carlisle, *Diamond Relat. Mater.* **14**, 86 (2005).
- ¹⁸R. J. Nemanich, J. T. Glass, G. Lucovsky, and R. E. Shroder, *J. Vac. Sci. Technol. A* **6**, 1783 (1988).
- ¹⁹F. J. Himpsel, J. A. Knapp, J. A. VanVechten, and D. E. Eastmann, *Phys. Rev. B* **20**, 624 (1979).
- ²⁰C. Bandis and B. B. Pate, *Phys. Rev. B* **52**, 12 056 (1995).
- ²¹J. van der Weide, Z. Zhang, P. K. Baumann, M. G. Wensell, J. Bernholc, and R. J. Nemanich, *Phys. Rev. B* **50**, 5803 (1994).
- ²²L. Diederich, O. M. Kuttel, E. Maillard-Schaller, and L. Schlapbach, *Surf. Sci.* **349**, 176 (1996).
- ²³P. K. Baumann and R. J. Nemanich, *Surf. Sci.* **409**, 320 (1998).
- ²⁴L. Diederich, O. M. Kuttel, P. Aebi, and L. Schlapbach, *Surf. Sci.* **418**, 219 (1998).
- ²⁵A. Modinos, *Field, Thermionic, and Secondary Electron Emission Spectroscopy* (Plenum Press, New York, 1984).
- ²⁶J. B. Cui, J. Ristein, and L. Ley, *Phys. Rev. Lett.* **81**, 429 (1998).
- ²⁷P. K. Baumann and R. J. Nemanich, *Surf. Sci.* **409**, 320 (1998).
- ²⁸S. A. Kajihara, A. Antonelli, J. Bernholc, and R. Car, *Phys. Rev. Lett.* **66**, 2010 (1991).